INTEGRATION OF IMMATURE NEURONS MAINTAIN UNIDIRECTIONAL CONNECTIVITY OF PRE-EXISTED NETWORK IN VITRO

V.N. Kolpakov[1,2], *M.S. Zemlyanskov*[1], *A.A. Gladkov*[1,2], *Y.I. Pigareva*[1,2], *A.S. Bukatin*[3,4], *V.B. Kazantsev*[1,2], *I.V. Mukhina*[1,2], *A.S. Pimashkin*[1,2*]

[1] Lobachevsky State University of Nizhny Novgorod, 23 Gagarina Pr., Nizhny Novgorod, 603950, Russia;
[2] Privolzhsky Research Medical University, 10/1 Minin and Pozharsky Sq., Nizhny Novgorod, 603005, Russia;
[3] Alferov Saint-Petersburg National Research Academic University of the Russian Academy of Sciences, 8/3 lit. A Khlopina St., Saint-Petersburg, 194021, Russia;
[4] Institute for Analytical Instrumentation of the RAS, 31-33 lit. A Ivana Chernykh St., Saint Petersburg, 198095, Russia.

* Corresponding author: pimashkin@neuro.nnov.ru

Abstract. Recovery of the neural networks after brain injury can be studied in vitro using cell patterning technologies such as microfluidics. In this study, neural tissue recovery of cortical networks was modeled in a three-chamber microfluidic chip by growing two weakly coupled neuronal networks and by plating new immature cells between it. The direction of synaptic connections was formed by the asymmetric design of the microchannels in the chip. We investigated dynamics of morphological characteristics of neurites growth through the microchannels and spiking activity propagation between the networks after integration of new cortical cells. The results can be used for the development of new approaches for brain functional recovery after injury.

Keywords: cultures of cortical neurons, microelectrode arrays, PDMS, microfluidic chips, axon guidance in microchannels, tissue engineering.

List of Abbreviations
PDMS – polydimethylsiloxane
MEA – multielectrode array
DIV – day in vitro

Introduction

Neuronal tissue repair and regeneration after brain injury is an important research topic in personalized medicine and Neuroscience which can be performed by implanting scaffold structures composed of various biodegradable materials with neuronal cells (Shimba *et al.*, 2019, Park *et al.*, 2019, Chai *et al.*, 2022, Jiang *et al.*, 2021). Modeling the recovery of connections between subnetworks *in vitro* allows the development of various strategies for treatment of nervous system diseases and injury recovery. It was shown that real-time hardware neuromorphic prosthesis based on electrical stimulation could restore bidirectional interactions between two neuronal populations *in vitro* (Buccelli *et al.*, 2019). Magnetically actuated micro robots directed the outgrowth of neurites and selectively connected separate neural clusters in vitro (Kim *et al.*, 2020). New connections between subnetworks could be formed using hydrogel threads (Kato-Negishi *et al.*, 2017) and soft microgels immersed in viscous extracellular-matrix solution (Kajtez *et al.*, 2020) loaded with neuronal cells. This approach is specified for modular 3D structures in which neuronal processes grow in both directions between modules. The brain has a heterogeneous network architecture with various types of cells and damaged neuronal networks must be replaced with similar architecture to restore functionality. Direction of cell neurite outgrowth must be precisely controlled when modeling the processes of restoring neural networks. Directional connections between subnetworks can be formed using asymmetric microchannels of microfluidic chips (Le Feber *et al.*, 2015; Na *et al.*, 2016; Holloway *et al.*, 2019; Courte *et al.*, 2018; Forró *et al.*, 2018; Moutaux *et al.*, 2018, Gladkov *et al.*, 2017). Previously, we presented an approach to restore network connections topology by integration of new cells between the fully-developed subnetworks (Shimba *et al.*, 2019). We hypothesized that a bridge through new integrated neurons was able to directly

connect two subnetworks by using microfluidic chips with microchannels for unidirectional axon growth and two-stage cell plating. Previously, we used a chip with three chambers with hippocampal neurons to test the concept (Kolpakov *et al.*, 2021). In vivo brain injury modeling and recovery are mostly studied in cortical areas of the brain (Shimba *et al.*, 2019, Park *et al.*, 2019, Chai *et al.*, 2022). Neuronal cells from various brain areas showed different neurite development dynamics (Dauth *et al.*, 2017). In this study we used a chip with three cell chambers to model weak synaptic connectivity in layered and feed-forward structure of the cortical network *in vitro*. Integration of new immature cortical cells in the region of axons between two subnetworks maintained defined functional connectivity. We analyzed the velocity of cortical neurite outgrowth in asymmetric microchannels and the propagation of spontaneous and stimulus-induced network activity.

Materials and Methods

Microfluidic microelectrode devise

Microfluidic chip microstructures were fabricated from polydimethylsiloxane (PDMS, Sylgard 184, USA) based on a template from our previous work (Kolpakov *et al.*, 2021), see it for details of chip fabrication. The chip had three cell chambers - Source, Implant and Target, connected as a forward chain by asymmetric microchannels for axons. There were 16 microchannels between the Source and Implant chambers and between the Implant and Target chambers. Wells for cell seeding were cut out manually using a blunt-tipped needle with an outer diameter of 1.8 mm.

For electrophysiological experiments microfluidic chips were aligned on the surface of a planar microelectrode array (MEA, Multichannel Systems, Germany) with 59 electrodes 30 mkm diameter at a distance of 200 μm arranged in an 8x8 grid. One line of microelectrodes was located in the cell chambers: 5, 8 and 6 electrodes in the chamber Source, Implant and Target respectively. The device was sterilized with 70% ethanol. After washing, it was covered with polyethyleneimine for 12 hours at 4°C.

Neuronal culture preparation

All experimental procedures were carried out following the protocol № 23 (31.10.2018) approved by the Bioethics Committee of the National Research Lobachevsky State University of Nizhny Novgorod (Russia). Cortexes of C57BL/6 mouse embryos at E18 were extracted and treated with trypsin (0.25%; Sigma, USA) for 20 min at 37°C. For details on this process see (Pigareva *et al.*, 2021). We loaded 4 μL of cell suspension with 20000 cells/μL in the chip chambers, so as to achieve a final plating density of about 7000-8000 cells/mm^2. Cells in the area of seeding wells were removed using a P10 pipette tip the next day after culture preparation. For experiments on the analysis of neurite growth along microchannels, the chips were attached to coverslips, and the cells were plated separately in identical chips only in one chamber Source or Implant or Target. Electrophysiological experiments with MEAs had two-stage planting of cells in three-chamber chips. At the first stage, cells were plated only into chambers Source and Target, and the Implant chamber remained empty. At the second stage (on 8th day in vitro (DIV)), new cells were plated into the Implant chamber (Fig. 1). For the control experiment 4 cultures remained without plating new cells and were studied to compare with others.

Electrophysiology

The multichannel registration system (Multichannel Systems, Germany) consisted of a connector, an amplifier, a data acquisition unit, a temperature controller, the STG-4004 stimulator, a computer, and software. Data was acquired at a sample rate of 20 kHz. MEA with chip and neuronal culture was taken out of the incubator and placed in the MEA connector, heated to 37 °C. Additionally, the connector with MEA was covered by a heating incubation chamber sustaining 5% CO_2 and 95% air. Experiments were carried out on 7-25 DIVs on 6 cultures. Before registration and stimulation sessions, MEA was left in the connector for 20 min to stabilize activity after mechanical disturbance due to movement. Then, 10 minutes of spontaneous activity were recorded.

Spike and burst detection methods were described in detail in a previous study (Pimashkin *et al.*, 2016). We estimated the probability of the burst propagation between subnetworks in chambers of the chip as the number of propagated bursts normalized to the total burst number in the network that was considered as a source of activity. See details in our previous study (Pigareva *et al.*, 2021). We estimated a ratio of forward/backward burst propagation between subnetworks in the chambers for each culture on 20 DIV.

Low-frequency stimulation consisted of 200 biphasic voltage pulses ±800 mV, 260 µs per phase, positive first, with 3s interstimulus intervals applied separately on two electrodes in the chambers Source, Implant, and Target independently. Electrical stimulation applied to the electrodes in the chambers evoked a response in the form of a network burst recorded by a group of electrodes. We estimated the number of evoked spikes at 10–300 ms intervals after each stimulus normalized to the number of recording electrodes. The number of evoked spikes was calculated separately for networks in the chamber Source, Implant, and Target. There were 6 stimulation experiments.

Imaging

The axon growth cone regions in the microchannels were observed using bright-field microscopy with Axio Observer.A1, Carl Zeiss, Germany. We analyzed neurite growing each day from 1 to 8 DIV (n = 48 microchannels, 3 chips). We processed and analyzed photos using the ImageJ program. We estimated the maximum daily distances that neurites grew in microchannels.

Statistical tests

All signal analysis and statistics were performed with custom-made software in Matlab (R).

Statistical significance was determined with a Mann-Whitney test.

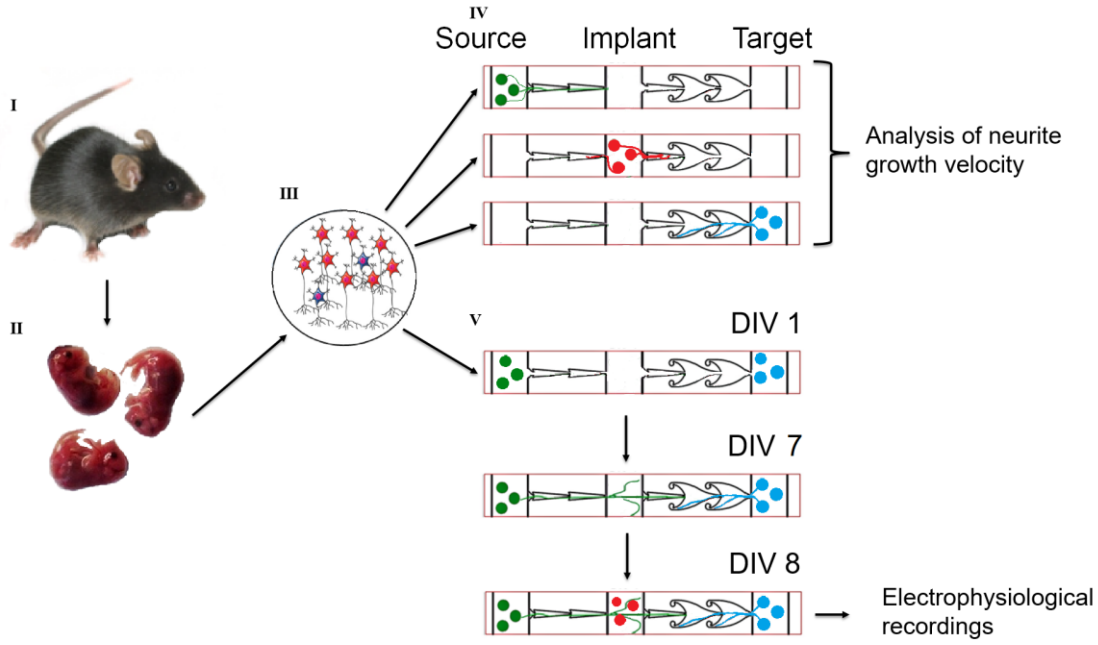

Fig. 1. Scheme of experiment: I – mouse line C57BL/6; II – E18 embryos; III – primary culture of neuronal cells; IV – experiment with analysis of axon growth in asymmetric microchannels; V – experiment with the integration of cells into a network with a unidirectional connection

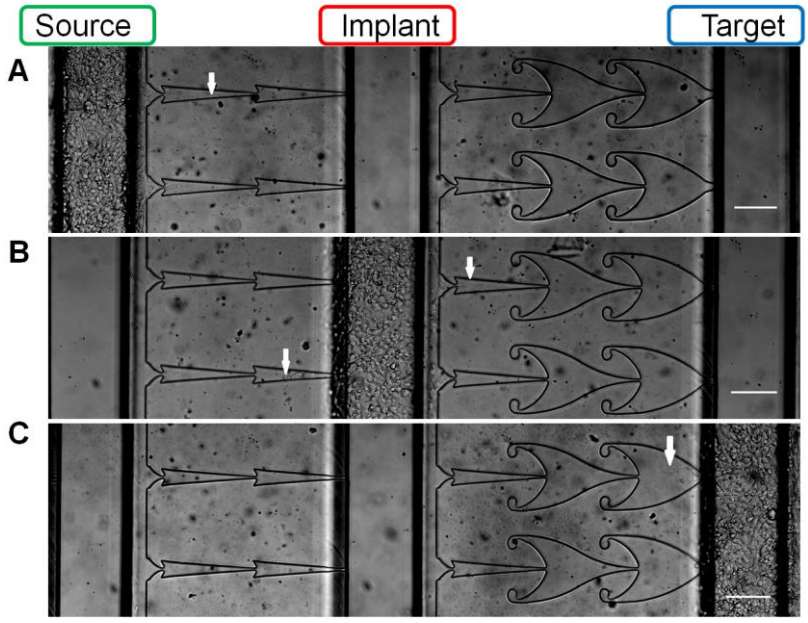

Fig. 2. Example photo of microchannels and chambers. In the presented example, the cortical cells were cultured (A) only in the Source chamber, (B) only in the Implant chamber, (C) only in the Target chamber (2 DIV). Group of neurites grow in microchannels (white arrows). Scale 100 μm

Results

Neurite growth analysis

First, we studied neurites of cultured cortical cells that grew through asymmetric microchannels of a 3-chamber chip in all possible directions: S-I, I-S, I-T, and T-I. We plated primary cortical cells only in one of three chambers of a microfluidic device. Within 48 h of culturing, the cortical cells started to form neurites that grew into the microchannels in all single chamber platings (Fig. 2). Daily image acquisition was used to monitor neurite growth velocity. We found that the neurites that originated from the chamber Source grew in the microchannels 84,5 ± 46,3 μм per day on the third DIV. The distribution of neurite growth velocity for microchannels between chambers Source and Implant is shown in Figure 3. Neurites that originated from the Implant chamber grew in the microchannels to the chamber Source 71.4 ± 27.5 μм per day on the third DIV. There were no differences for these microchannels (n = 48, Mann-Whitney test, $p > 0.05$). The neurite growth velocity in microchannels on the third day from the Implant chamber to the Target chamber was higher than from the Target cham-ber to the Implant (n = 48, Mann-Whitney test, $p < < 0.05$), 113.4 ± 40.2 μm /day and 69.6 ± ± 24.5 μm/day, respectively (Fig. 4).

Analysis of spontaneous bioelectrical activity

Cultured cortical networks displayed synchronous bursting activity after 10 days *in vitro*. We studied the propagation of network bursts between subnetworks in the chambers of a microfluidic device in experiments with two-stage cell planting (see Methods). The propagation probability of spontaneous network bursts from the Source to the Implant was higher than from the Implant to the Source, 52.83 ± 22.21% and 7.34 ± 13.85%, respectively (Fig. 5). The propagation probability of spontaneous network bursts from the Implant to the Target was higher than from the Target to the Implant, 52.83 ± 22.21% and 7.34 ± 13.85%, respectively. The propagation probability in the forward direction from the Source to the Target was also higher than in the opposite direction from the Target to the Source 51.53 ± 25.63% and 0.99 ± 1.96%, respectively (mean ± standard deviation, Mann-

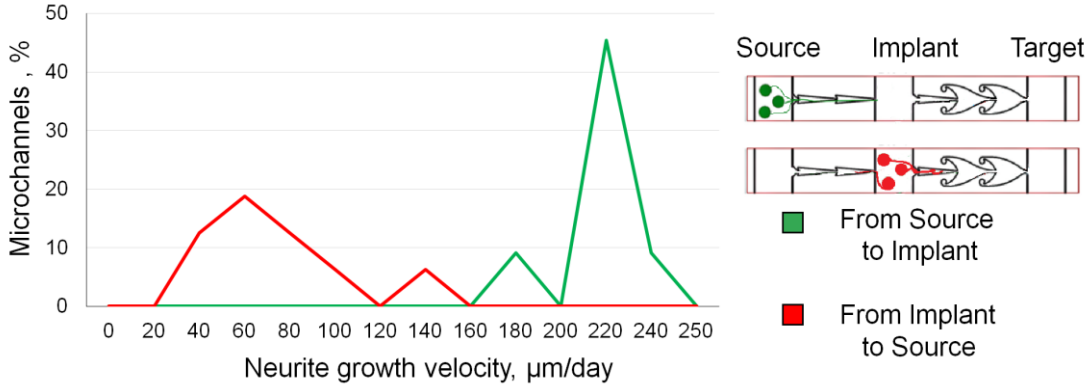

Fig. 3. The distribution of neurite growth velocity in microchannels between the Source and Implant chambers on 3 DIV. A schematic representation of the microchannel is in the upper right corner

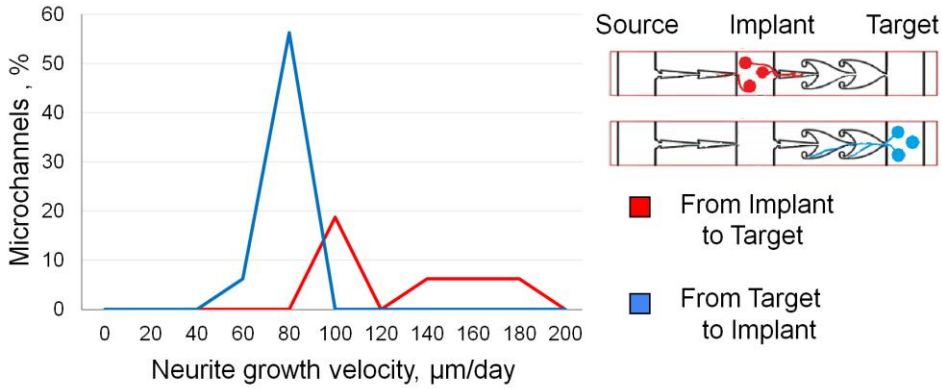

Fig. 4. The distribution of the neurite growth velocity in microchannels between the Implant and Target on 3 DIV. A schematic representation of the microchannel is in the upper right corner

Whitney test, $p < 0.001$; n = 14 experiments on three cultures with two-stage plating of cells). To compare cultures with integrated cells to control cultures we estimated a ratio of forward/backward burst propagation between subnetworks in the Source and Target for each culture on 20 DIV. Preliminary results show that the ratio for cultures with integrated cells was 4.72 ± 2.08 (n = 3 cultures) compared to cultures without integration, 3.12 ± 2.29 (n = 4 cultures). The ratio of forward/backward burst propagation did not differ for control experiments and with integration of new cells (Mann-Whitney test, $p > 0.05$). Propagation probability of spontaneous bursts from Implant to Source and from Source to Implant did not differ for control experiments and with integration of new cells on 20 DIV, forward: 40.5 ± 29.8% and 61.3 ± 27.0%, backward: 11.25 ± 6.29% and 14.0 ± 5.57%, respectively.

Analysis of stimulus-evoked activity

Low-frequency electrical stimuli of one of the subnetworks in the microfluidic device evoked a spiking response in the stimulated subnetwork and in neighboring connected subnetworks. We estimated the number of spikes in the time interval from 10 to 300 ms after the stimulus separately in each subnetwork when one of the subnetworks was stimulated. The number of evoked spikes was different in each subnetwork when they were stimulated (Mann-Whitney test with Bonferroni adjustment, $p << 0.001$, n = 6 experiments, 3 cultures with two-stage cell plating). As shown in Figure 6, when the stimulation electrode was in the Target

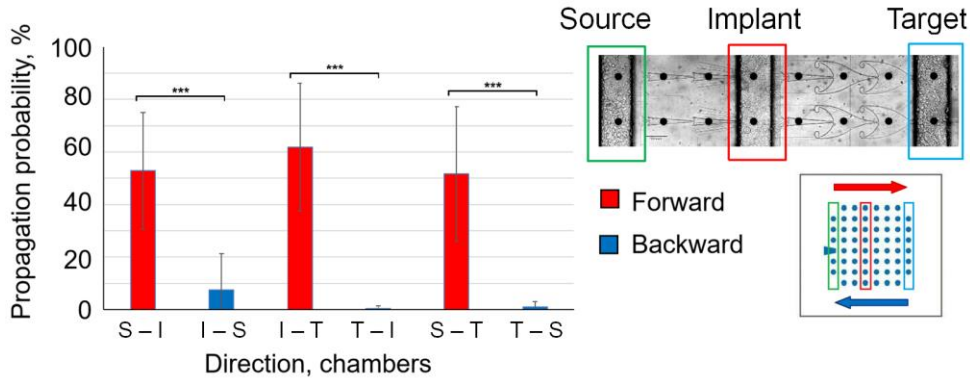

Fig. 5. The probability of propagation of spontaneous bursting activity between the neural subnetworks in the chambers Source (S), Implant (I), Target (T) (Mann-Whitney test, $p < 0.001$; $n = 14$ experiments); in the right, a schematic representation of the microelectrode array and a photograph of the neuronal culture, showing the location of the electrodes in the chambers and microchannels

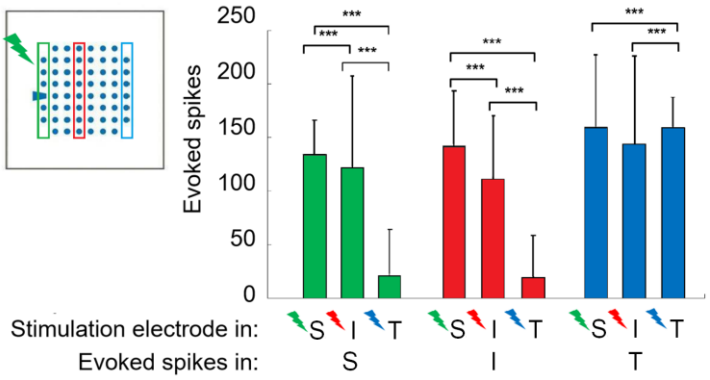

Fig. 6. The number of evoked spikes after stimulus in one of the chambers: green – in the Source chamber (S); red – in the Implant chamber (I); blue – in the Target chamber (T). Chambers with a stimulated electrode are marked with the corresponding lightning color (Mann-Whitney test with Bonferroni correction, $p < 0.001$, $n = 6$ experiments)

chamber the number of evoked spikes in the Source and Implant were lower than the number of spikes in all chambers when stimulation electrodes were in the Source and Implant. Thus, the evoked bioelectrical activity propagated between all subnetworks. The propagation of evoked network activity was dominantly from the subnetworks in the Source and Implant chambers to the subnetwork in the Target chamber, but not in the opposite direction.

Discussion

In this study, we investigated a three-chamber chip platform to study spiking activity changes after the integration of the cortical cells into weakly coupled cultured cortical neural networks *in vitro*. The method was based on a previously proposed experimental model (Kolpakov *et al.*, 2021) and was performed using cortical cells. Functional restoration of cortical networks is an important area to study brain repair after injury or disease treatment (Shimba *et al.*, 2019, Park *et al.*, 2019, Chai *et al.*, 2022) The number of axons that could grow through microchannels is limited by the total cross-sectional area (Pan *et al.*, 2015). The different growth velocity of neurites in microchannels in the forward and the opposite directions leads to forming unidirectional connections between subnetworks. We observed a predominant growth of neurites in a defined direction in cultured neural networks of the neocortex, sim-

ilar to the networks of the hippocampus in our previous studies (Kolpakov *et al.*, 2021). Here, for the first time, we analyzed the neurite growth velocity in asymmetric microchannels of the three-chamber chip. The shape of the microchannels of the microfluidic chip provided a higher neurite growth velocity in the forward direction than in the reverse direction during the first week of development of the cortical cell culture. The directionality of the connections between neural networks in the Source and Implant chambers could be formed due to a delay in cell plating (DeMasrse *et al.*, 2016). At the same time, plating cells first in the Target chamber and then in the Implant with a delay of several days promotes preferential growth and spread of activity from the Target to the Implant. The design of microchannels with axon traps has been proposed to avoid the effect of plating delay. Microchannels with axon traps created conditions for a directed connection from new cells in the Implant chamber to a mature cortical network in the Target chamber with a plating delay for at least 8 days.

The analysis of the spontaneous activity of the networks showed that the probability of network bursts propagation in the forward direction is significantly higher than in the opposite direction. New cells plated in Implant chamber on 8 DIV functionally integrated between the cultures, didn't disrupt network integrity, maintained unidirectional synaptic connectivity and transmitted spontaneous spiking activity from Source to Target chambers.

The analysis of the stimulus evoked activity showed that the number of evoked spikes in the Source and Implant chambers after stimulus applying to the Target chamber is significantly lower than the number of spikes in all chambers when stimulation electrodes are in the Source and Implant chambers. The microfluidic chip provides high accuracy of cell integration in the area of directional connection between two subnetworks of neuronal cells. The chip is compatible with standard commercial microelectrode arrays and allows non-invasive study of the electrophysiological characteristics of each subnetwork. The experimental platform can be used to model multilayer feed-forward structure of neocortex and simulate recovery or enhancement of the functional connectivity after brain injury.

Funding: this work was supported by the Russian Science Foundation, grant No. 21-75-10154.

References

BUCCELLI S., BORNAT Y., COLOMBI I., AMBROISE M., MARTINES L., PASQUALE V., BISIO M., TESSADORI J., ŁAW NOWAK P., GRASSIA F., AVERNA A., TEDESCO M. T., BONIFAZI P., DIFATO F., MASSOBRIO P., LEVI T. & CHIAPPALONE M. (2019): A neuromorphic prosthesis to restore communication in neuronal networks. *IScience* **19**, 402–414.

CHAI Y., ZHAO H., YANG S., GAO X., CAO Z., LU J., ... & WANG X. (2022). Structural alignment guides oriented migration and differentiation of endogenous neural stem cells for neurogenesis in brain injury treatment. *Biomaterials* **280**, 121310.

COURTE J., RENAULT R., JAN A., VIOVY J.L., PEYRIN J.M. & VILLARD C. (2018): Reconstruction of directed neuronal networks in a microfluidic device with asymmetric microchannels. In: *Methods in cell biology* (Vol. 148), pp. 71–95. Academic Press.

DAUTH S., MAOZ B.M., SHEEHY S.P., HEMPHILL M.A., MURTY T., MACEDONIA M.K., ... & PARKER K.K. (2017). Neurons derived from different brain regions are inherently different in vitro: a novel multiregional brain-on-a-chip. *Journal of neurophysiology* **117**(3), 1320–1341.

DEMARSE T.B., PAN L., ALAGAPAN S., BREWER G.J. & WHEELER B.C. (2016): Feed-forward propagation of temporal and rate information between cortical populations during coherent activation in engineered *in vitro* networks. *Frontiers in neural circuits* **10**, 32.

EPIFANOVA E., BABAEV A., NEWMAN A.G. & TARABYKIN V. (2019): Role of Zeb2/Sip1 in neuronal development. *Brain Research* **1705**, 24–31.

FORRÓ C., THOMPSON-STECKEL G., WEAVER S., WEYDERT S., IHLE S., DERMUTZ H., AEBERSOLD M.J., PILZ R., DEMKÓ L. & VÖRÖS J. (2018): Modular microstructure design to build neuronal networks of defined functional connectivity. *Biosensors and Bioelectronics* **122**, 75–87.

JIANG J., DAI C., LIU X., DAI L., LI R., MA K., ... & ZHANG S. (2021). Implantation of regenerative complexes in traumatic brain injury canine models enhances the reconstruction of neural networks and motor function recovery. *Theranostics* **11**(2), 768.

HABIBEY R., ROJO ARIAS J.E., STRIEBEL J. & BUSSKAMP V. (2022): Microfluidics for Neuronal Cell and Circuit Engineering. *Chemical Reviews* **122**(18), 14842–14880.

HOLLOWAY P.M., HALLINAN G.I., HEGDE M., LANE S.I., DEINHARDT K. & WEST J. (2019): Asymmetric confinement for defining outgrowth directionality. *Lab on a Chip* **19**(8), 1484–1489.

KAJTEZ J., WESSELER M.F., BIRTELE M., KHORASGANI F.R., RYLANDER OTTOSSON D., HEISKANEN A., KAMPERMAN T., LEIJTEN J., MARTÍNEZ-SERRANO A., LARSEN N.B., ANGELINI T.E., PARMAR M., LIND J.U. & EMNÉUS J. (2022): Embedded 3D Printing in Self-Healing Annealable Composites for Precise Patterning of Functionally Mature Human Neural Constructs. *Advanced Science* **9**(25), 2201392.

KATO-NEGISHI M., ONOE H., ITO A. & TAKEUCHI S. (2017): Rod-shaped neural units for aligned 3D neural network connection. *Advanced Healthcare Materials* **6**(15), 1700143.

KIM E., JEON S., AN H.K., KIANPOUR M., YU S.W., KIM J.Y., RAH J-C. & CHOI H. (2020): A magnetically actuated microrobot for targeted neural cell delivery and selective connection of neural networks. *Science advances* **6**(39), eabb5696.

KOLPAKOV V.N., PIGAREVA Y.I., GLADKOV A.A., BUKATIN A.S., KAZANTSEV V.B., MUKHINA I.V. & PIMASHKIN A.S. (2021): Model of 'implant-host'neural circuits in a microfluidic chip in vitro. In *Journal of Physics: Conference Series* (Vol. 2086, No. 1), p. 012111. IOP Publishing.

LE FEBER J., POSTMA W., DE WEERD E., WEUSTHOF M. & RUTTEN W.L. (2015): Barbed channels enhance unidirectional connectivity between neuronal networks cultured on multi electrode arrays. *Frontiers in neuroscience* **9**, 412.

MOUTAUX E., CHARLOT B., GENOUX A., SAUDOU F. & CAZORLA M. (2018): An integrated microfluidic/microelectrode array for the study of activity-dependent intracellular dynamics in neuronal networks. *Lab on a Chip* **18**(22), 3425–3435.

NA S., KANG M., BANG S., PARK D., KIM J., SIM S.J., CHANG S. & JEON N.L. (2016): Microfluidic neural axon diode. *Technology* **4**(04), 240–248.

PAN L., ALAGAPAN S., FRANCA E., LEONDOPULOS S.S., DEMARSE T.B., BREWER G. J. & WHEELER B.C. (2015): An *in vitro* method to manipulate the direction and functional strength between neural populations. *Frontiers in neural circuits* **9**, 32.

PARK J.B., SUNG D., PARK S., MIN K.A., KIM K.W., CHOI Y., ... & LEE D.S. (2019). 3D graphene-cellulose nanofiber hybrid scaffolds for cortical reconstruction in brain injuries. *2D Materials* **6**(4), 045043.

PIGAREVA Y., GLADKOV A., KOLPAKOV V., MUKHINA I., BUKATIN A., KAZANTSEV V.B. & PIMASHKIN A. (2021): Experimental platform to study spiking pattern propagation in modular networks in vitro. *Brain Sciences* **11**(6), 717.

PIMASHKIN A., GLADKOV A., AGRBA E., MUKHINA I. & KAZANTSEV V. (2016): Selectivity of stimulus induced responses in cultured hippocampal networks on microelectrode arrays. *Cognitive neurodynamics* **10**(4), 287–299.

ROS O. & NICOL X. (2022): Axon pathfinding and targeting:(R) evolution of insights from in vitro assays. *Neuroscience*.

SHIMBA K., CHANG C.H., ASAHINA T., MORIYA F., KOTANI K., JIMBO Y., ... & PIMASHKIN A. (2019): Functional scaffolding for brain implants: engineered neuronal network by microfabrication and iPSC technology. *Frontiers in Neuroscience* **13**, 890.

YE X., QIU Y., GAO Y., WAN D. & ZHU H. (2019): A subtle network mediating axon guidance: intrinsic dynamic structure of growth cone, attractive and repulsive molecular cues, and the intermediate role of signaling pathways. *Neural Plasticity*, 2019.